Eur. Phys. J. C (2022) 82:161
https://doi.org/10.1140/epjc/s10052-022-10055-z

THE EUROPEAN PHYSICAL JOURNAL C

Regular Article - Theoretical Physics

Hunting for the heavy quark spin symmetry partner of Z_{cs}

Xu Cao[1,2,a], **Zhi Yang**[3,b]

[1] Institute of Modern Physics, Chinese Academy of Sciences, Lanzhou 730000, China
[2] University of Chinese Academy of Sciences, Beijing 100049, China
[3] School of Physics, University of Electronic Science and Technology of China, Chengdu 610054, China

Received: 20 October 2021 / Accepted: 25 January 2022 / Published online: 21 February 2022

Abstract The discovery of a charged strange hidden-charm state $Z_{cs}(3985)$ implies another higher Z_{cs}^* state coupling to $\bar{D}_s^{*-}D^{*0}+c.c$ under the heavy quark spin symmetry. In this paper we discuss a possible hunt for it with data taken at existing facilities. We point out a hint for Z_{cs}^* in the data of $\bar{B}_s^0 \to J/\psi K^- K^+$ at LHCb, though weak, in line with the production mechanism of pentaquark P_c. We also study the triangular singularity which would possibly enhance the production of Z_{cs}^* in electron-positron collision. Surprisingly, the production rate of Z_{cs}^* is expected to be maximum at the e^+e^- center of mass energy of 4.648 GeV, which is lower than 4.681 GeV for Z_{cs} due to the inverted coupling hierarchy of $D_{s1}\bar{D}^*K$ and $D_{s2}\bar{D}K$ in the triangle diagrams. Their bottom analogue under heavy quark flavor symmetry is also discussed. Our theoretical analysis would confront with future experiment of LHCb, BESIII, and Bell II.

1 Introduction

The evidence of strange pentaquark $P_{cs}(4459)$ from LHCb Collaboration [1], though only 3σ significance, marked the dawn of strange era for the exploration of exotic candidates. Soon afterwards the BESIII collaboration discovered a charged resonance with the significance of more than 5σ in the $D_s^- D^{*0} + D_s^{*-} D^0$ mass distribution of $e^+e^- \to K^+(D_s^- D^{*0} + D_s^{*-} D^0)$, whose mass and width are [2]

$$Z_{cs}(3985): \quad 3982.5^{+1.8}_{-2.6} \pm 2.1\,\text{MeV}, \quad 12.8^{+5.3}_{-4.4} \pm 3.0\,\text{MeV}$$

It is close to the $D_s^- D^{*0}$ and $D_s^{*-} D^0$ thresholds with the probable quantum number being $J^P = 1^+$. This motivates its interpretation of $D_s^- D^{*0} + D_s^{*-} D^0$ molecular state as the strange partner of $Z_c(3900)$ in various scenarios, e.g. in QCD sum rules before [3,4] and after its observation [5–12]. Its inner structure and mass spectra are extensively investigated in hadro-quarkonium [13] and compact tetraquark models [14], and various quark models, for instance, the chiral quark model [15,16], the dynamical diquark model [17,18], the model with meson-meson and diquark-antidiquark constituents [19,20]. Its decays of hidden charm [21] and open charm [22] channels, configuration mixing [23] and compositeness [24] are also studied.

Whether one-Boson-exchange potential is strong enough to bind $D_s^- D^{*0}$ and $D_s^{*-} D^0$ is inconclusive in the coupled channel formalism after considering the OZI suppression [25–27]. Other binding mechanisms for molecular explanation are under investigation, e.g. contact interaction [28–34], axial-meson exchange [35], and channel recoupling mechanism [36]. Under SU(3)-flavor symmetry, its existence is definitely expected as the strange partner of $Z_c(3900)$, theorized to be isovector $D^*\bar{D}^*$ molecular. Another higher strange axial-vector state $Z_{cs}(4130)$ of $D_s^*\bar{D}^*$ component (labeled as Z_{cs}^* hereafter), as strange partner of $Z_c^*(4020)$ of $D^*\bar{D}^*$ molecular nature, is predicted in many scenarios [28,29,34,37]. So a complete multiplet under heavy quark flavor and spin symmetry (HQFS and HQSS) is emerging after the evident twin molecules $Z_c(3900)$ and $Z_c(4020)$ in hidden charm sector [38–41], and their close analogs $Z_b(10610)$ and $Z_b(10650)$ in hidden bottom sector [40].

In QCD sum rule [4], initial K-meson emission mechanism [22], and hadrocharmonium picture [13], hidden-charm channels are anticipated to be essential for understanding the $Z_{cs}(3985)$. However, $e^+e^- \to J/\psi K^- K^+$ is not statistically achievable at present [42–44]. Recent data of $B^+ \to J/\psi\phi K^+$ from the LHCb Collaboration reveals the existence of two wide charged strange hidden-charm states in the $J/\psi K^+$ spectrum [45]. The Breit-Wigner (BW) masses and widths are, respectively

$$Z_{cs}(4000): \quad 4003 \pm 6^{+4}_{-14}\,\text{MeV}, \quad 131 \pm 15 \pm 26\,\text{MeV}$$
$$Z_{cs}(4220): \quad 4216 \pm 24^{+43}_{-30}\,\text{MeV}, \quad 233 \pm 52^{+97}_{-73}\,\text{MeV}$$

[a] e-mail: caoxu@impcas.ac.cn
[b] e-mail: zhiyang@uestc.edu.cn (corresponding author)

These Z_{cs} states are unambiguously assigned to be $J^P = 1^+$ states. The masses of $Z_{cs}(3985)$ and $Z_{cs}(4000)$ are consistent within uncertainties, motivating the hypothesis of them as one state [28,46]. In this case, the $Z_{cs}(4220)$ would be an excited state of $Z_{cs}(3985)$. If considering them as two different states, the $Z_{cs}(3985) \to J/\psi K$ decay is suppressed in the limit of the HQSS [47], and the $Z_{cs}(4220)$ at LHCb would be the expected axial-vector $D_s^* \bar{D}^*$ molecular. Instead, the Z_{cs}^* is predicted to be a $D_s^* \bar{D}^*$ resonance of tensor 2^+ nature with mass of about 4126 MeV and width of 13 MeV. In both schemes a narrow Z_{cs}^* close to $D_s^* \bar{D}^*$ threshold plays a central role. In Sec. 2 a weak hint is shown for this state in the data of $\bar{B}_s^0 \to J/\psi K^- K^+$ at LHCb. A wide $Z_{cs}(4250)$, consistent with $Z_{cs}(4220)$ at LHCb, is predicted by HQSS within hadroquarkonium framework [13] together with another $Z_{cs}(4350)$ as the respective partners of $Z_c(4100)$ [48] and $Z_c(4200)$ [49] (for a discussion of their spin-parity see [50]).

In electron-positron collision, kinematic effects, e.g. triangle singularity (TS) [22,28] and kinematic reflection [51] are thought to play an important role. When all the intermediate particles in a triangle diagram move collinearly on their mass shell a triangle singularity happens to mimic the resonance-like peak in the invariant mass distributions [52]. The width of particles in triangle diagrams of B-decay would induce the wide Z_{cs} at LHCb [53], explaining the $Z_{cs}(3985)/Z_{cs}(4220)$ width difference. It is possible to distinguish TS mechanism by searching for the photo- [54] and lepto-production [55] and pion/kaon induced reactions [56] of exotic mesons, because the on-shell condition is hardly satisfied in these reactions [57,58]. On the other hand, the triangle diagram possess a triangle singularity under a special energy, hence it becomes an amplifier of the production of exotic candidates in certain energies as experiments found. The $Z_c(3900)$ signal is enhanced by the $D_1 \bar{D}^0 D^*$ triangle diagram when the e^+e^- center of mass (c.m.) energy is around Y(4260), close to the $D_1 \bar{D}^0$ threshold [59]. Analogously the $D_{s2}(2573) \bar{D}_s^* D^0$ triangle diagram would enhance the production of $Z_{cs}(3985)$ at c.m. energy of 4.681 GeV [28]. Considering that the $D_{s1}(2536)$ is approximately the HQSS partner of the $D_{s2}(2573)$, we point out in Sec. 3 that the production of predicted axial-vector Z_{cs}^* would be magnified by the $D_{s1}(2536) \bar{D}_s^* D^{*0}$ triangle around $D_{s1}(2536) \bar{D}_s^*$ threshold.

2 A hint of Z_{cs}^* at $\bar{B}_s$-decay

The hidden-charm pentaquark states P_c with the same light quark content as the nucleon are discovered in $\Lambda_b \to J/\psi K^- p$ by LHCb collaboration [61,62]. Based on SU(3)-flavor symmetry, the bottom baryon decay would be decomposed into the internal and external W-emission diagrams [63]. The three quarks $c\bar{c}s$ produced directly from the b-quark

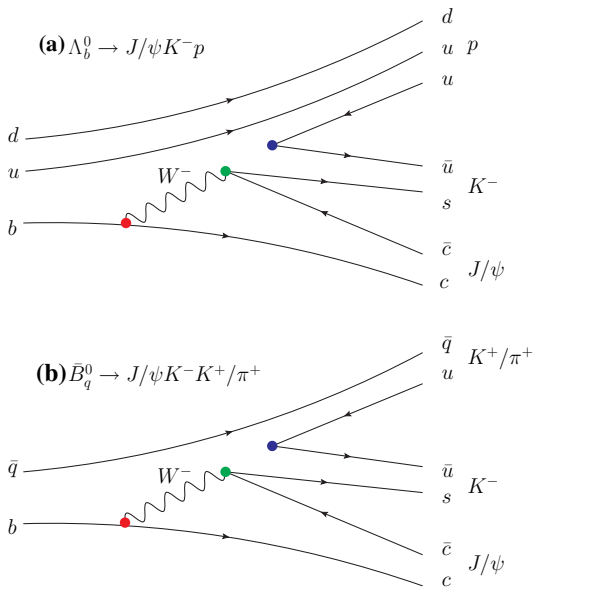

Fig. 1 Internal W-emission in (a) the $\Lambda_b \to J/\psi K^- p$ decay, and (b) the $\bar{B}^0 \to J/\psi K^- \pi^+$ and $\bar{B}_s^0 \to J/\psi K^- K^+$. The diagram for the charge conjugate channel of $B^+ \to J/\psi \phi K^+$ can be obtained with $u\bar{u} \to s\bar{s}$ in (b)

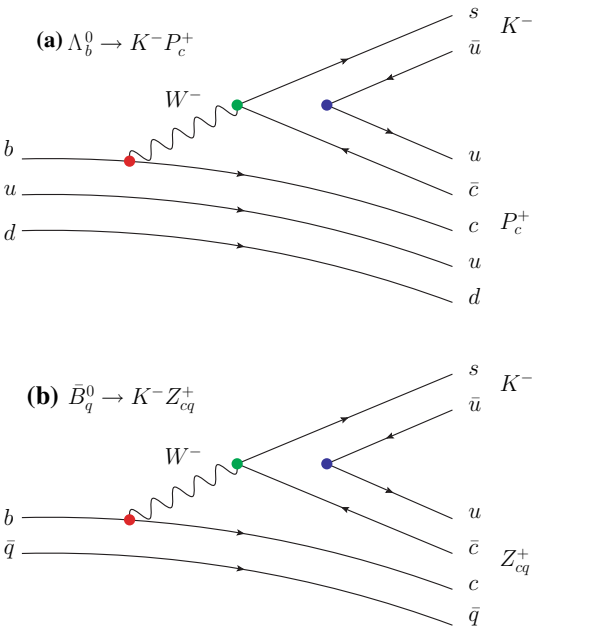

Fig. 2 Exotic states production by external W-emission in (a) the $\Lambda_b \to P_c^+ K^-$ decay, and (b) the $\bar{B}^0 \to Z_c^+ K^- \pi^+$ and $\bar{B}_s^0 \to Z_{cs}^{(*)} K^-$. The diagram for the charge conjugate channel of $B^+ \to Z_{cs}^+ \phi$ can be obtained with $u\bar{u} \to s\bar{s}$ in (b)

decay by the internal W-emission in Fig. 1(a) are too energetic to form a bound pentaquark. The dominant pentaquark production process is anticipated to be the external W-emission amplitudes in Fig. 2(a) [63]. The close analogous diagrams for bottom meson decays are shown in Fig. 1(b) and Fig. 2(b) for $\bar{B}^0 \to J/\psi K^- \pi^+$ and $\bar{B}_s^0 \to J/\psi K^- K^+$.

Table 1 Parameters of contact interaction and poles of $Z_{cs}^{(*)}$ taken from Ref. [28]. Results outside (inside) brackets are for cutoff Λ = 0.5 GeV (1 GeV), respectively

	Virtual	Resonant
$C^{(O)}$ (fm^2)	$-0.77^{+0.12}_{-0.10}$ $\left(-0.45^{+0.05}_{-0.04}\right)$	$-0.72^{+0.18}_{-0.13}$ $\left(-0.44^{+0.06}_{-0.05}\right)$
$D^{(O)}$ (fm^4)	-	$-0.17^{+0.21}_{-0.21}$ $\left(-0.025^{+0.066}_{-0.049}\right)$
Z_{cs} (MeV)	3974^{+2}_{-3} $\left(3971^{+3}_{-6}\right)$	$3963^{+15}_{-5} - i3^{+17}_{-3}$ $\left(3966^{+13}_{-31} - i0^{+31}_{-0}\right)$
Z_{cs}^{*} (MeV)	4117^{+3}_{-5} $\left(4115^{+3}_{-6}\right)$	$4110^{+11}_{-5} - i0^{+15}_{-0}$ $\left(4111^{+10}_{-23} - i0^{+28}_{-0}\right)$

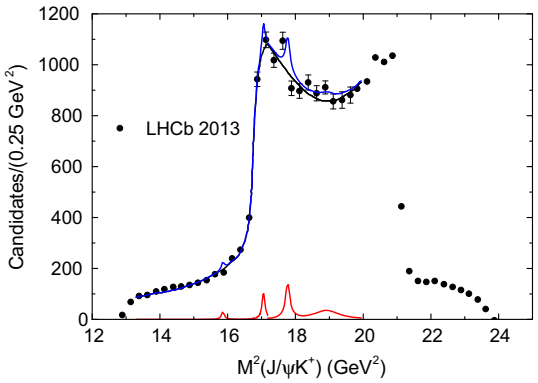

Fig. 3 The data of $J/\psi K^+$ spectrum in $\bar{B}_s^0 \to J/\psi K^- K^+$ at LHCb [60] and the possible contribution of $Z_{cs}(3985)$, $Z_{cs}^*(4130)$, $Z_{cs}(4220)$ and $Z_{cs}(4350)$. The red curves are Breit-Wigner (BW) distributions of those Z_{cs}. Here the central values of mass and width from BESIII are used for $Z_{cs}(3985)$. The central values of mass from LHCb is used for $Z_{cs}(4220)$ with a width of 20.0 MeV. The mass and width of $Z_{cs}^*(4130)$ are respectively 4130 MeV and 15 MeV as expected by HQSS and SU(3)-flavor symmetry [5,29,47]. The mass of $Z_{cs}(4350)$ is quoted from hadro-quarkonium [13] and width 100 MeV is adopted. The blue solid curve is the incoherent sum of BW and simulated background mainly reflected from $K^- K^+$ spectrum by LHCb

The $Z_c(4200)$ and $Z_c(4600)$ are already discovered in the former decay by LHCb [49,64], supporting that this argument of production mechanism is similarly applicable for bottom meson decays. Another decay of this beneficial feature is $B^+ \to J/\psi\phi K^+$, in which two wide Z_{cs} appeared after considerably increasing statistics at LHCb [45] in comparison with previous measurements [65–69]. So it seems that $\bar{B}_s^0 \to J/\psi K^- K^+$ deserve further search for Z_{cs} production though it bears low statistics at present [60]. Current data of this decay at LHCb in Fig. 3 shows none clue for $Z_{cs}(3985)/Z_{cs}(4000)$, but does hint weakly for Z_{cs}^* and $Z_{cs}(4220)$, both of which are narrow. Another wide 4350 MeV can be accommodated, but its signal is even more fuzzy. Due to the wide energy bins (500 MeV) of the data, their evidence is rather inconclusive.

In an isospin analysis of $B \to D^* \bar{D} K$ it is shown that the production of the isospin triplet state $Z_c(3900)$ is highly suppressed in B decays compared to the isospin singlet $X(3872)$ [70]. As the strange partner of $Z_c(3900)$, $Z_{cs}(3985)$ would be also absent in the open-channel B decays by isospin suppression. Similar TS as discussed in $B^+ \to J/\psi\phi K^+$ [53] would also raise the width of $Z_{cs}(3985)$ and Z_{cs}^* to be around 100 MeV, making them hard to appear in B- and $\bar{B}_s$-decays. But the masses in the triangles are demanding for TS due to the fixed masses of mother particles B/B_s.

Considering the branching ratios $\mathcal{B}(\bar{B}^0 \to J/\psi K^- \pi^+) = (1.15 \pm 0.05) \times 10^{-3}$, $\mathcal{B}(B^+ \to J/\psi\phi K^+) = (5.0 \pm 0.4) \times 10^{-5}$, and $\mathcal{B}(\bar{B}_s^0 \to J/\psi K^- K^+) = (2.54 \pm 0.35) \times 10^{-6}$ [71], increase of the accumulated statistics by around 20 times at least would induce the refined discovery of Z_{cs}^* and others.

3 Triangle diagrams in e^+e^- annihilation

The BEPCII continues to run for collecting integrated luminosity at different energies so BESIII provides the chance to look for Z_{cs}^* in e^+e^- annihilation. In an effective field theory, the production of $Z_c(3900/4020)$ and $Z_{cs}(3985)$ are dynamically understandable in a consistent manner with the help of Lippmann-Schwinger equation — $T = V + VG_0T$, where V denotes the potential and G_0 is the two-point loop function. For explicit expressions, we refer to Ref. [28,59] within the nonrelativistic approximation. The contact-range interaction incorporating the SU(3)-flavor symmetry contains at most two low-energy constants (LECs) at leading order [28],

$$V_{\text{virtual}}^{(O)} = C^{(O)}(\Lambda)\,. \tag{1}$$

$$V_{\text{res}}^{(O)} = C^{(O)}(\Lambda) + 2D^{(O)}(\Lambda)\,k^2\,, \tag{2}$$

with k the c.m. momentum of the two mesons. The momentum independent kernel in Eq. (1) generates a bound or a virtual pole below its respective two-meson threshold, while the latter in Eq. (2) generates a resonant state. Here Λ means that the divergent loop function G_0 has been regulated by a Gaussian form factor $e^{-(p/\Lambda)^2}$ with p the momentum of the two mesons in e^+e^- system. The values of LECs can be determined by the masses and widths of $Z_c(3900/4020)$ and $Z_{cs}(3985)$, as summarized in Table 1 together with the generated poles of $Z_{cs}^{(*)}$.

In this framework, the $D_1\bar{D}^0D^*$ triangle diagram, as part of the generation of the $Z_c(3900)$ signal, enhances its produc-

tion when the e^+e^- center of mass (c.m.) energy is around $Y(4260)$, close to the $D_1\bar{D}^0$ threshold [59]. Analogously the $D_{s2}(2573)\bar{D}_s^* D^0$ triangle diagram, contributing to the generation of $Z_{cs}(3985)$ as shown in Fig. 4(a), would enhance the production of $Z_{cs}(3985)$ at the c.m. energy of 4.681 GeV [28]. Note that $D_{s2}D\bar{K}$ decay proceeds in D-wave. Considering that the $D_{s1}(2536)$ is approximately the HQSS partner of the $D_{s2}(2573)$, Fig. 5(a) with $D_{s1}(2536)\bar{D}_s^* D^{*0}$ triangle is a close analog of Fig. 4(a). The scalar 3-point loop integral of these diagrams is given by [41,72,73]

$$I = \frac{\mu_{12}\mu_{23}}{2\pi\sqrt{a}}\left[\arctan\left(\frac{c_2 - c_1}{2\sqrt{a(c_1 - i\epsilon)}}\right) - \arctan\left(\frac{c_2 - c_1 - 2a}{2\sqrt{a(c_2 - a - i\epsilon)}}\right)\right], \tag{3}$$

where μ_{12} and μ_{23} are the reduced masses of the $D_{s1}\bar{D}_s^*$ and $\bar{D}_s^* D^{*0}$, respectively, $a = \left(\mu_{23} q_K / m_{D^{*0}}\right)^2$, $c_1 = 2\mu_{12} b_{12}$, $c_2 = 2\mu_{23} b_{23} + q_K^2 \mu_{23}/m_{D^{*0}}$ with $b_{12} = m_{D_{s1}} + m_{\bar{D}_s^*} - \sqrt{s}$ and $b_{23} = m_{\bar{D}_s^*} + m_{D^{*0}} + E_K - \sqrt{s}$, and $q_K(E_K)$ is the K^+ momentum (energy) in the γ^* c.m. frame. The involved

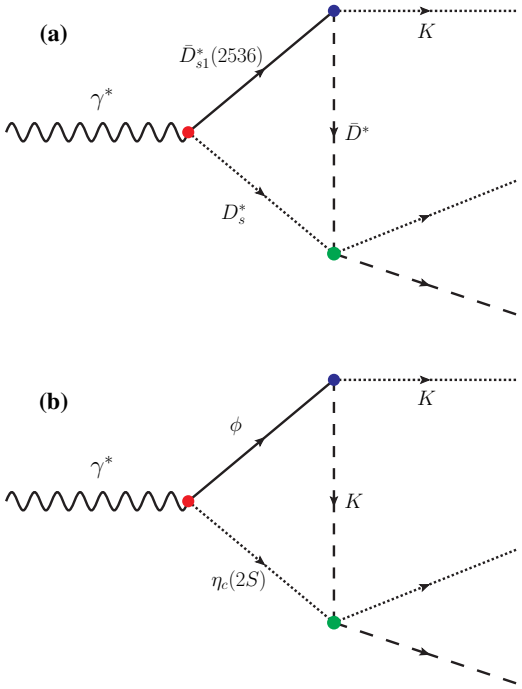

Fig. 4 Possible (a) $D_{s2}(2573)\bar{D}_s^* D^0$ and (b) $J/\psi f_2'(1525)K^*$ triangle diagrams of $e^+e^- \to K^+ Z_{cs}(3985)$ process with the generated $Z_{cs}(3985)$ (green circles) decaying to $D_s^- D^{*0}$, $D_s^{*-} D^0$, $J/\psi K$ or other possible channels. The blue vertices are all in D-wave here. The green circles denote the T-matrix elements which include the effects of the generated $Z_{cs}(3985)$ state

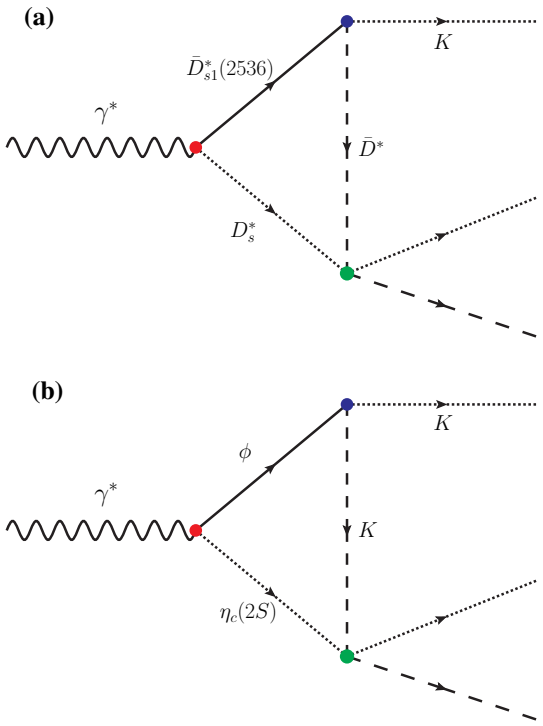

Fig. 5 Possible (a) $D_{s1}(2536)\bar{D}_s^* D^{*0}$ and (b) $\eta_c \phi K$ triangle diagrams of $e^+e^- \to K^+ Z_{cs}^*$ process with the generated Z_{cs}^* (green circles) decaying to $\bar{D}_s^* D^0$, $J/\psi K$ or other possible channels. The green circles denote the T-matrix elements which include the effects of the generated Z_{cs}^* state

kinematic variables are given by

$$\begin{aligned} q_K &= \frac{1}{2M}\sqrt{\lambda(s, m_K^2, m_{23}^2)}, \\ m_{13}^2 &= m_K^2 + m_{D^{*0}}^2 + 2E_1^* E_3^* - 2p_1^* p_3^* \cos\theta_3^*, \\ p_1^* &= \sqrt{E_1^{*2} - m_K^2}, \quad p_3^* = \frac{1}{2m_{23}}\sqrt{\lambda(m_{23}^2, m_2^2, m_3^2)}, \\ E_3^* &= \frac{m_{23}^2 - m_2^2 + m_3^2}{2m_{23}}, \quad E_1^* = \frac{s - m_{23}^2 - m_K^2}{2m_{23}}, \end{aligned} \tag{4}$$

where $m_2 = m_{D_s^*}$ and $m_3 = m_{D^{*0}}$.

Fig. 6 shows the absolute value squared of the corresponding scalar triangle loop integral $|I|^2$ at the e^+e^- c.m. energy of 4.648 GeV, around the $D_{s1}\bar{D}_s^*$ threshold. Quite close results are obtained for different input of parameters from Table 1. Data are needed to constrain the relative normalization of the different amplitudes, so at present the $m_{\bar{D}_s^* D^{*0}}$ spectrum can not be predicted. However, after convolution with the three-body phase space of $e^+e^- \to \bar{D}_s^* D^{*0} K^+$ a clear peak around 4.12 GeV appears to enhance the production of axial vector Z_{cs}^*. The Z_{cs}^* of tensor nature is suppressed in this mechanism due to its involvement of D-wave at least for the total production amplitudes, so it serves a possible experimental criteria of Z_{cs}^* with J^P. Interestingly $\gamma^* D_{s1}\bar{D}_s^*$

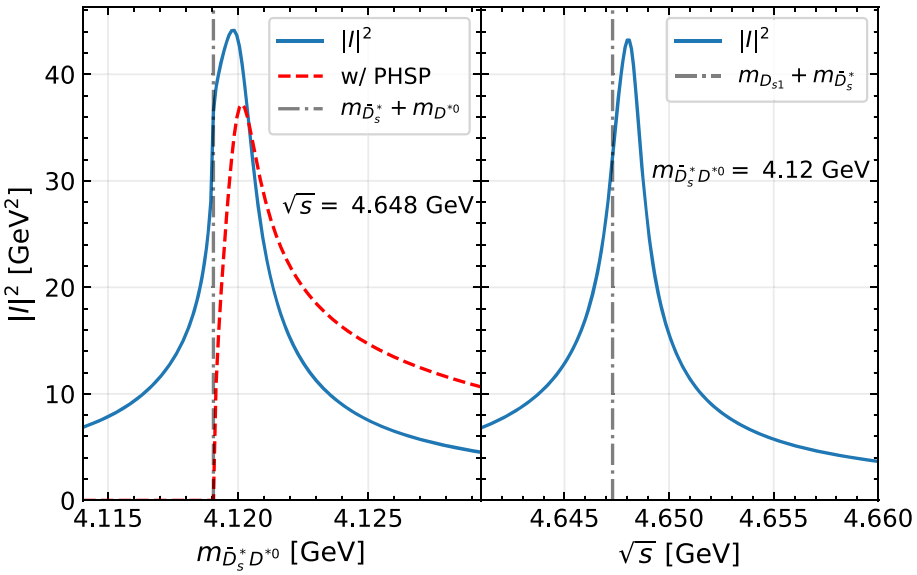

Fig. 6 Absolute squared value of the scalar triangle loop integral, $|I|^2$, with the $D_{s1}\bar{D}_s^* D^{*0}$ triangle diagram shown as Fig. 5(a). Left: dependence on the $\bar{D}_s^* D^{*0}$ invariant mass for $\sqrt{s} = 4.648$ GeV, where we also show $|I|^2$ convoluted with the phase space, with the maximum normalized to that of $|I|^2$; right: dependence on $\sqrt{s}$ with $m_{\bar{D}_s^* D^{*0}} = 4.12$ GeV

vertex in D-wave results into 33.0 MeV lower c.m. energy of Z_{cs}^* production than that of the $Z_{cs}(3985)$. This is due to the inverted coupling hierarchy of $D_{s1}\bar{D}^* K$ and $D_{s2}\bar{D}K$. Here the inverted hierarchy refers to the fact that the D_{s2} is heavier than the D_{s1}, however the D_{s2} decays mainly to $\bar{D}K$ which is lighter than the dominant decay channel $\bar{D}^* K$ of the D_{s1}. Unfortunately BEPCII scans the c.m. energies with 20 MeV interval, and its best luminosities are at 4.640 and 4.660 GeV, a little shift from the best energy to identify the contribution of triangle diagrams. The Bell experiment collects a large data sample at or near the Υ resonances in e^+e^- collision, with the possibility to search for the $Z_{cs}^{(*)}$ state through initial-state radiation [74].

The $D_{s2}\bar{D}_s^* D^*$ triangle diagram can also develop a triangle singularity contributing to the production of Z_{cs}^*. Its HQSS correspondence $D_{s1}\bar{D}_s^* D$ would present to the production of $Z_{cs}(3985)$. We ignore them for two reasons. First, up to now the $D_{s2} \to D^* K$ decay and its HQSS correspondence $D_{s1} \to DK$, both in D-wave, are not found by experiment, so their couplings are expected to be small. Second, the $D_{s2}\bar{D}_s^* D^*$ triangle diagram would induce a singularity at e^+e^- c.m. energy of 4.685 GeV, around the $D_{s2}\bar{D}_s^*$ threshold. Under this energy $Z_{cs}(3985)$ is produced but Z_{cs}^* not, as BESIII found. This seems to support the former point. Another place to explore these kind of triangle diagrams is $K^* Z_{cs}^{(*)}$ channels, i.e. $e^+e^- \to K^*(\bar{D}_s^{(*)} D^* + \bar{D}_s^* D^{(*)})$. However, the decay $D_{s1}(D_{s2}) \to D^{(*)} K^*$ is not found at present and higher e^+e^- c.m. energies due to K^* mass are expected to be out of the reach of the BESIII and other available facilities. Moreover, experimentally the K^* reconstruction is more difficult and needs much more integrated luminosity.

Other triangle diagrams are possibly present in the production of $Z_{cs}^{(*)}$ in e^+e^- annihilation. For the $Z_{cs}(3985)$, a triangle of $J/\psi f_2'(1525) K^*$ in Fig. 4(b) has singularity in c.m. energy of around 4622 MeV. Due to the 86 ± 5 MeV width of $f_2'(1525)$ and its moderate coupling of $K^*\bar{K}$, the enhancement would not so sharp and is possibly submerged by the smooth background. No enhancement of $Z_{cs}(3985)$ production in the $e^+e^- \to K^+(D_s^- D^{*0} + D_s^{*-} D^0)$ data of BESIII at 4628 MeV seems to support these arguments [2]. Similarly the $\eta_c(2S)\phi K$ triangle in Fig. 5(b) would contribute to the Z_{cs}^* production with all vertices in p-wave. The narrow width of $\eta_c(2S)$ and strong coupling of ϕ to $K\bar{K}$ would enhance the Z_{cs}^* production at c.m. energy of 4657 MeV, about 10 MeV above that of Fig. 5(a). However, the $Z_{cs}^{(*)}$ in the molecular scenario mainly decay to open charm channels $\bar{D}_s^{(*)} D^{*0} + D_s^* \bar{D}^{(*)}$, so the T-matrix elements denoted by green circles in Figs. 4 and 5 generate $Z_{cs}^{(*)}$ state in the elastic channel. Both Figs. 4(b) and 5(b) are disadvantage of the inelastic interaction of hidden charm $J/\psi K^*$ or $\eta_c(2S)K$ vertices in $e^+e^- \to K^+(\bar{D}_s^{(*)} D^{*0} + D_s^* \bar{D}^{(*)})$.

As a result, $D_{s2}(2573)\bar{D}_s^* D^0$ and $D_{s1}(2536)\bar{D}_s^* D^{*0}$ triangle diagrams are anticipated to be the dominant singularity for the $Z_{cs}(3985)$ and Z_{cs}^* production, respectively. Their correspondence in bottom sector is quite similar. The $Z_b(10610)$ and $Z_b(10650)$ (Z_b and Z_b^*) discovered a decade ago by the Belle collaboration, are a pair of charged hidden-bottom resonances with $I^G(J^{PC}) = 1^-(1^{+-})$ and masses [75]

$$M(Z_b^{\pm}) = 10607.2 \pm 2.0\,\text{MeV}\,, \tag{5}$$
$$M(Z_b^{*\pm}) = 10652.2 \pm 1.5\,\text{MeV}\,, \tag{6}$$

very close to the $B\bar{B}^*$ and $B^*\bar{B}^*$ thresholds, respectively. Their strange partners are predicted to be close to the $B_s\bar{B}^* + B_s^*\bar{B}$ and $B_s^*\bar{B}^*$ thresholds [5,28,29,54]:

$$M(Z_{bs}^{\pm}) \simeq 10700\,\text{MeV}\,, \tag{7}$$
$$M(Z_{bs}^{*\pm}) \simeq 10745\,\text{MeV}\,, \tag{8}$$

if the Z_b's were indeed bound states of the bottom mesons mentioned above. Considering that the dominant decays are $B_{s1}(5830) \to B^*K$ and $B_{s2}(5840) \to BK$, the $B_{s2}(5840)\bar{B}_s^* B$ and $B_{s1}(5830)\bar{B}_s^* B^*$ triangle diagrams are anticipated to be the dominant singularity for the Z_{bs} and Z_{bs}^* production in e^+e^- annihilation, respectively. The inverted c.m. energy gap for their production is only about 10 MeV due to the mass difference between $B_{s1}(5830)$ and $B_{s2}(5840)$.

4 Summary and Conclusion

The $Z_{cs}(3985)$ state, together with the $X_0(2900)$ and $X_1(2900)$ of quark content $\bar{c}\bar{s}ud$ by LHCb [76,77], raised the question of existence of a complete exotic spectrum of the charm and charm-strange. A missing piece of this molecule jigsaw puzzle is Z_{cs}^* as expected by HQSS and SU(3)-flavor symmetry. Inspired by the dominance of external W-emission, in this paper we call attention to a hint for Z_{cs}^* production by the same mechanism in the data of $\bar{B}_s^0 \to J/\psi K^- K^+$ at LHCb, which needs further investigation with higher statistics. We further explore the triangular singularity which would possibly enhance the production of axial-vector Z_{cs}^* state in $e^+e^- \to K^{*+} D_s^{*-} D^{*0}$. The Z_{cs}^* is expected to be enhanced by the $D_{s1}(2536)\bar{D}_s^* D^{*0}$ triangle diagrams, similar to that of $D_{s2}(2573)\bar{D}_s^* D^0$ for $Z_{cs}(3985)$ production in e^+e^- annihilation. As a surprising result, Z_{cs}^* would be produced in about 30 MeV lower c.m. energy of e^+e^- than that of Z_{cs}, due to the inverted coupling hierarchy of $D_{s1}\bar{D}^* K$ and $D_{s2}\bar{D}K$. Their bottom partners are analogous with a relative smaller energy gap of e^+e^- between Z_{bs} and Z_{bs}^* production. Our results are helpful for the future hunt for Z_{cs}^* in $\bar{B}_s$-decay and e^+e^- annihilation.

The same mechanism in e^+e^- annihilation is considered within similar framework in Ref. [78], which incorporates the whole energy range covered by the BESIII data by including more channels and triangle diagrams. One of the fits in Ref. [78] is a global minimum fit and agrees with our scenario, as addressed in Ref. [78]. Another local minimum incorporates a strong coupled-channel effects between $\bar{D}_s^* D^*$ ($\bar{D}^* D^*$) and $\bar{D}_s D^* + \bar{D}_s^* D$ ($\bar{D} D^* + \bar{D}^* D$), which generate only one fine-tuned bound state $Z_{cs}(3985)$ ($Z_c(3900)$) without the accommodation of Z_{cs}^* ($Z_c(4020)$). Both $D_{s1,2}\bar{D}_s^{(*)} D^*$ triangle diagrams are important for $Z_{cs}(3985)$ production in this case but we argue that the couplings of $D_{s2}D^*K$ and $D_{s1}DK$ seem to be weak. This study supports our motivation of this paper that hunting for Z_{cs}^* is essential for distinguishing different mechanisms. A experimental study of the e^+e^- c.m. energy of 4.648 GeV would be very helpful because Z_{cs}^* would not be present around 4.648 GeV in latter fit of Ref. [78], contrary to our prediction here.

Acknowledgements We would like to thank Juan Nieves, Manuel Pavon Valderrama, Feng-Kun Guo and Jian-Ping Dai for useful communication. This work is supported by the National Natural Science Foundation of China (Grants Nos. 12075289, 11847301, and U2032109) and the Strategic Priority Research Program of Chinese Academy of Sciences (Grant NO. XDB34030301). This work was supported by Fundamental Research Funds for the Central Universities (2019CDJDWL0005).

Data Statement This manuscript has no associated data or the data will not be deposited. [Authors' comment: All data generated or analyzed during this theoretical study are included in this published article.]

Funded by SCOAP[3].

References

1. R. Aaij et al. (LHCb), Sci. Bull. **66**, 1391 (2021). arXiv:2012.10380
2. M. Ablikim et al. (BESIII), Phys. Rev. Lett. **126**, 102001 (2021). arXiv:2011.07855
3. S.H. Lee, M. Nielsen, U. Wiedner, J. Korean Phys. Soc. **55**, 424 (2009). arXiv:0803.1168
4. J.M. Dias, X. Liu, M. Nielsen, Phys. Rev. D **88**, 096014 (2013). arXiv:1307.7100
5. B. Wang, L. Meng, S.-L. Zhu, Phys. Rev. D **103**, L021501 (2021). arXiv:2011.10922
6. U. Ozdem, A.K. Yildirim, Phys. Rev. D **104**, 054017 (2021). arXiv:2104.13074
7. U. Özdem, K. Azizi, Eur. Phys. J. Plus **136**, 968 (2021). arXiv:2102.09231
8. Z.-G. Wang, Chin. Phys. C **45**, 073107 (2021). arXiv:2011.10959
9. K. Azizi, N. Er, Eur. Phys. J. C **81**, 61 (2021). arXiv:2011.11488
10. Z.-G. Wang, Int. J. Mod. Phys. A **36**, 2150107 (2021). arXiv:2012.11869
11. Y.-J. Xu, Y.-L. Liu, C.-Y. Cui, M.-Q. Huang, Phys. Rev. D **104**, 094028 (2021). arXiv:2011.14313
12. B.-D. Wan, C.-F. Qiao, Nucl. Phys. B **968**, 115450 (2021). arXiv:2011.08747
13. M.B. Voloshin, Phys. Lett. B **798**, 135022 (2019). arXiv:1901.01936
14. J. Ferretti, E. Santopinto, JHEP **04**, 119 (2020). arXiv:2001.01067
15. G. Yang, J. Ping, J. Segovia, Phys. Rev. D **104**, 094035 (2021). arXiv:2109.04311
16. X. Chen, Y. Tan, Y. Chen, Phys. Rev. D **104**, 014017 (2021). arXiv:2103.07347
17. J.F. Giron, R.F. Lebed, S.R. Martinez, Phys. Rev. D **104**, 054001 (2021). arXiv:2106.05883
18. P.-P. Shi, F. Huang, W.-L. Wang, Phys. Rev. D **103**, 094038 (2021). arXiv:2105.02397
19. X. Jin, Y. Wu, X. Liu, Y. Xue, H. Huang, J. Ping, B. Zhong, Eur. Phys. J. C **81**, 1108 (2021). arXiv:2011.12230

20. D. Ebert, R.N. Faustov, V.O. Galkin, Eur. Phys. J. C **58**, 399 (2008). arXiv:0808.3912
21. Q. Wu, D.-Y. Chen, Phys. Rev. D **104**, 074011 (2021). arXiv:2108.06700
22. D.-Y. Chen, X. Liu, T. Matsuki, Phys. Rev. Lett. **110**, 232001 (2013). arXiv:1303.6842
23. M. Karliner, J.L. Rosner, Phys. Rev. D **104**, 034033 (2021). arXiv:2107.04915
24. Z.-H. Guo, J.A. Oller, Phys. Rev. D **103**, 054021 (2021). arXiv:2012.11904
25. Z.-F. Sun, C.-W. Xiao (2020). arXiv:2011.09404
26. R. Chen, Q. Huang, Phys. Rev. D **103**, 034008 (2021). arXiv:2011.09156
27. Z.-M. Ding, H.-Y. Jiang, D. Song, J. He, Eur. Phys. J. C **81**, 732 (2021). arXiv:2107.00855
28. Z. Yang, X. Cao, F.-K. Guo, J. Nieves, M.P. Valderrama, Phys. Rev. D **103**, 074029 (2021). arXiv:2011.08725
29. L. Meng, B. Wang, S.-L. Zhu, Phys. Rev. D **102**, 111502 (2020). arXiv:2011.08656
30. N. Ikeno, R. Molina, E. Oset, Phys. Lett. B **814**, 136120 (2021). arXiv:2011.13425
31. X.-K. Dong, F.-K. Guo, B.-S. Zou, Phys. Rev. Lett. **126**, 152001 (2021). arXiv:2011.14517
32. X.-K. Dong, F.-K. Guo, B.-S. Zou, Commun. Theor. Phys. **73**, 125201 (2021). arXiv:2108.02673
33. X.-K. Dong, F.-K. Guo, B.-S. Zou, Prog. Phys. **41**, 65 (2021). arXiv:2101.01021
34. M.-C. Du, Q. Wang, Q. Zhao (2020). arXiv:2011.09225
35. M.-J. Yan, F.-Z. Peng, M. Sánchez Sánchez, M. Pavon Valderrama, Phys. Rev. D **104**, 114025 (2021). arXiv:2102.13058
36. Y.A. Simonov, JHEP **04**, 051 (2021). arXiv:2011.12326
37. K. Zhu, Int. J. Mod. Phys. A **36**, 2150126 (2021). arXiv:2101.10622
38. J. Nieves, M.P. Valderrama, Phys. Rev. D **86**, 056004 (2012). arXiv:1204.2790
39. C. Hidalgo-Duque, J. Nieves, M.P. Valderrama, Phys. Rev. D **87**, 076006 (2013). arXiv:1210.5431
40. F.-K. Guo, C. Hidalgo-Duque, J. Nieves, M.P. Valderrama, Phys. Rev. D **88**, 054007 (2013). arXiv:1303.6608
41. F.-K. Guo, C. Hanhart, U.-G. Meißner, Q. Wang, Q. Zhao, B.-S. Zou, Rev. Mod. Phys. **90**, 015004 (2018). arXiv:1705.00141
42. C.Z. Yuan et al. (Belle), Phys. Rev. D **77**, 011105 (2008). arXiv:0709.2565
43. C.P. Shen et al. (Belle), Phys. Rev. D **89**, 072015 (2014). arXiv:1402.6578
44. M. Ablikim et al. (BESIII), Phys. Rev. D **97**, 071101 (2018). arXiv:1802.01216
45. R. Aaij et al. (LHCb), Phys. Rev. Lett. **127**, 082001 (2021). arXiv:2103.01803
46. P.G. Ortega, D.R. Entem, F. Fernandez, Phys. Lett. B **818**, 136382 (2021). arXiv:2103.07871
47. L. Meng, B. Wang, G.-J. Wang, S.-L. Zhu, Sci. Bull. **66**, 1516 (2021). arXiv:2104.08469
48. R. Aaij et al. (LHCb), Eur. Phys. J. C **78**, 1019 (2018). arXiv:1809.07416
49. K. Chilikin et al. (Belle), Phys. Rev. D **90**, 112009 (2014). arXiv:1408.6457
50. X. Cao, J.-P. Dai, Phys. Rev. D **100**, 054004 (2019). arXiv:1811.06434
51. J.-Z. Wang, Q.-S. Zhou, X. Liu, T. Matsuki, Eur. Phys. J. C **81**, 51 (2021). arXiv:2011.08628
52. F.-K. Guo, X.-H. Liu, S. Sakai, Prog. Part. Nucl. Phys. **112**, 103757 (2020). arXiv:1912.07030
53. Y.-H. Ge, X.-H. Liu, H.-W. Ke, Eur. Phys. J. C **81**, 854 (2021). arXiv:2103.05282
54. X. Cao, J.-P. Dai, Z. Yang, Eur. Phys. J. C **81**, 184 (2021). arXiv:2011.09244
55. Z. Yang, F.-K. Guo, Chin. Phys. C **45**, 123101 (2021). arXiv:2107.12247
56. J. Liu, D.-Y. Chen, J. He, Eur. Phys. J. C **81**, 965 (2021). arXiv:2108.00148
57. X.-H. Liu, M. Oka, Nucl. Phys. A **954**, 352 (2016). arXiv:1602.07069
58. X. Cao, J.-P. Dai, Phys. Rev. D **100**, 054033 (2019). arXiv:1904.06015
59. M. Albaladejo, F.-K. Guo, C. Hidalgo-Duque, J. Nieves, Phys. Lett. B **755**, 337 (2016). arXiv:1512.03638
60. R. Aaij et al. (LHCb), Phys. Rev. D **87**, 072004 (2013). arXiv:1302.1213
61. R. Aaij et al. (LHCb), Phys. Rev. Lett. **115**, 072001 (2015). arXiv:1507.03414
62. R. Aaij et al. (LHCb), Phys. Rev. Lett. **122**, 222001 (2019). arXiv:1904.03947
63. H.-Y. Cheng, C.-K. Chua, Phys. Rev. D **92**, 096009 (2015). arXiv:1509.03708
64. R. Aaij et al. (LHCb), Phys. Rev. Lett. **122**, 152002 (2019). arXiv:1901.05745
65. R. Aaij et al. (LHCb), Phys. Rev. Lett. **118**, 022003 (2017). arXiv:1606.07895
66. R. Aaij et al. (LHCb), Phys. Rev. D **95**, 012002 (2017). arXiv:1606.07898
67. T. Aaltonen et al. (CDF), Phys. Rev. Lett. **102**, 242002 (2009). arXiv:0903.2229
68. T. Aaltonen et al. (CDF), Mod. Phys. Lett. A **32**, 1750139 (2017). arXiv:1101.6058
69. S. Chatrchyan et al. (CMS), Phys. Lett. B **734**, 261 (2014). arXiv:1309.6920
70. Z. Yang, Q. Wang, U.-G. Meißner, Phys. Lett. B **775**, 50 (2017). arXiv:1706.00960
71. P. A. Zyla et al. (Particle Data Group), PTEP **2020**, 083C01 (2020)
72. F.-K. Guo, C. Hanhart, G. Li, U.-G. Meissner, Q. Zhao, Phys. Rev. D **83**, 034013 (2011). arXiv:1008.3632
73. F.-K. Guo, Nucl. Phys. Rev. **37**, 406 (2020). arXiv:2001.05884
74. W. Altmannshofer et al. (Belle-II), PTEP **2019**, 123C01 (2019). arXiv:1808.10567. [Erratum: PTEP **2020**, 029201 (2020)]
75. A. Bondar et al. (Belle), Phys. Rev. Lett. **108**, 122001 (2012). arXiv:1110.2251
76. R. Aaij et al. (LHCb), Phys. Rev. Lett. **125**, 242001 (2020). arXiv:2009.00025
77. R. Aaij et al. (LHCb), Phys. Rev. D **102**, 112003 (2020). arXiv:2009.00026
78. V. Baru, E. Epelbaum, A.A. Filin, C. Hanhart, A.V. Nefediev (2021). arXiv:2110.00398